

Drop impact in the regime of film boiling : transient evolution of the heat transfer and the vapor film thickness

Guillaume Castanet, William Chaze, Ophelie Caballina, Romain Collignon, Fabrice Lemoine

▶ **To cite this version:**

Guillaume Castanet, William Chaze, Ophelie Caballina, Romain Collignon, Fabrice Lemoine. Drop impact in the regime of film boiling : transient evolution of the heat transfer and the vapor film thickness. 29th Conference on Liquid Atomization and Spray Systems, Sep 2019, Paris, France. hal-02388412

HAL Id: hal-02388412
https://hal.science/hal-02388412

Submitted on 1 Dec 2019

HAL is a multi-disciplinary open access archive for the deposit and dissemination of scientific research documents, whether they are published or not. The documents may come from teaching and research institutions in France or abroad, or from public or private research centers.

L'archive ouverte pluridisciplinaire **HAL**, est destinée au dépôt et à la diffusion de documents scientifiques de niveau recherche, publiés ou non, émanant des établissements d'enseignement et de recherche français ou étrangers, des laboratoires publics ou privés.

Drop impact in the regime of film boiling : transient evolution of the heat transfer and the vapor film thickness

Guillaume Castanet[1], William Chaze[1], Ophélie Caballina[1,*], Romain Collignon[1], Fabrice Lemoine[1]
[1]Université de Lorraine, CNRS, LEMTA, F-54000 Nancy, France
*Corresponding author: ophelie.caballina@univ-lorraine.fr

Abstract
When a drop impinges onto a wall heated above the Leidenfrost temperature, a very thin vapor film is formed at the interface between the liquid and the solid substrate. This vapor layer modifies the impact behavior of the drop and induces a significant decrease in heat transfer. To study this phenomenon, a model is proposed for the growth of the vapor film and the heat transfer at the impact. The main assumptions are: (i) a uniform but time varying thickness of the vapor film, (ii) a quasi-steady Poiseuille flow inside the vapor film, and (iii) a constant wall temperature. Heat energy and momentum balances are employed to obtain an ordinary differential equation describing the evolution of the vapor film thickness during the drop impact. Upon a one-dimensional analysis (nonetheless including some effects due to the complex fluid flow), the local heat flux transferred to the liquid q_L can be evaluated. When the initial drop temperature is sufficiently lower than the saturation temperature, q_L predominates over the heat flux used for liquid evaporation. This results in a simplified model for the vapor film thickness that we were able to validate against experiments carried out with ethanol droplets impacting an overheated sapphire surface (typically above 250℃). Two optical measurement techniques, based on laser-induced fluorescence imaging and infrared thermography, are associated to temporally and spatially characterize the heat transfer as well as the thickness of the vapor film.

Keywords
Film boiling, Drop impact, Vapor film thickness.

Introduction

Cooling of hot surfaces by sprays, drops or droplets is common in many applications, such as in the quenching of hot metals [1, 2], or in the cooling of power electronics [3]. It has driven the attention of many researchers because of the ability of sprays to remove high quantities of heat using limited mass flow rates of liquid coolant. However, while spray cooling has been applied for decades, its integration remains complex due to ill understanding of the heat transfer characteristics of spray cooling. Correlations for the heat transfer coefficient are generally determined experimentally on a global scale, based on the mean parameters of the spray (for example the mean size and velocity of the impinging droplets). Such correlations can serve well for an intended application, but in general they poorly perform whenever the configuration of the spray is changed. There is therefore an important need to obtain a glimpse of the underlying physics, which implies investigating the fundamental case of the impact of a single droplet. Numerous studies have focused on the impact of a single droplet onto an isothermal surface, which does not require consideration of heat transfer and phase change. The emphasis was mainly placed on the drop behavior evaluating the diameter and the velocity of the outcoming droplets (partial/total rebound, splashing) [4], the spreading of the liquid film [5]. These investigations mainly aimed at determining the influence of the dynamics of the impinging droplet (velocity, diameter...), the physical properties of the liquid (viscosity, surface tension...) and of the solid surface (surface roughness, wettability...) on the impact process. All these works must be reexamined carefully when the wall is heated above the boiling point of the liquid. Even when the temperature of the solid substrate exceeds the saturation temperature of the liquid by a few degrees, boiling can considerably change the droplet behavior. As for pool boiling, the heat flux is a complex non-monotonic function of the wall temperature. From the boiling curve, heat transfer during drop impingement can be categorized into boiling regimes: (i) natural convection boiling, (ii) nucleate boiling, (iii) transition boiling and (iv) film boiling. At very high substrate temperatures, in the regime of film boiling, the liquid does not remain in contact with the solid. A vapor layer is formed underneath the droplet and prevent at any time a direct contact between the liquid and the solid surface, which is hugely detrimental to heat transfer. The main subject of the present study is the introduction of a predictive theoretical model for heat transfer during drop impact in the film boiling regime. Some theoretical models are available for sessile droplets, deposited without velocity on the solid surface. Biance et al. [6] derived some scaling laws for the vapor film thickness. They evidenced distinctive evolution of the vapor thickness depending on whether the droplet size exceeds or not the capillary length. Sobac et al. [7] proposed a model based upon lubrication theory which accounts for the curvature of the liquid/vapor interface. This approach provides good agreements with experimental works showing the presence of a vapor pocket underneath the droplet and a neck in the vapor film profile. However, these theoretical approaches are difficult to adapt to the case of a drop impact, since liquid inertia considerably modifies the force acting upon the vapor film and the spreading evolution of the droplet. Recently, Breitenbach et al. [8] derived a theoretical model to predict the heat transferred from the hot substrate to the single drop during impact. They considered a uniform but time variable thickness of the vapor film and they proposed an explicit expression for the thickness of the vapor layer obtained from the energy balance at the liquid-vapor and vapor-solid interfaces. A significant difference with the present study, however, concerns the heat flux used for liquid

This work is licensed under a Creative Commons 4.0 International License (CC BY-NC-ND 4.0).

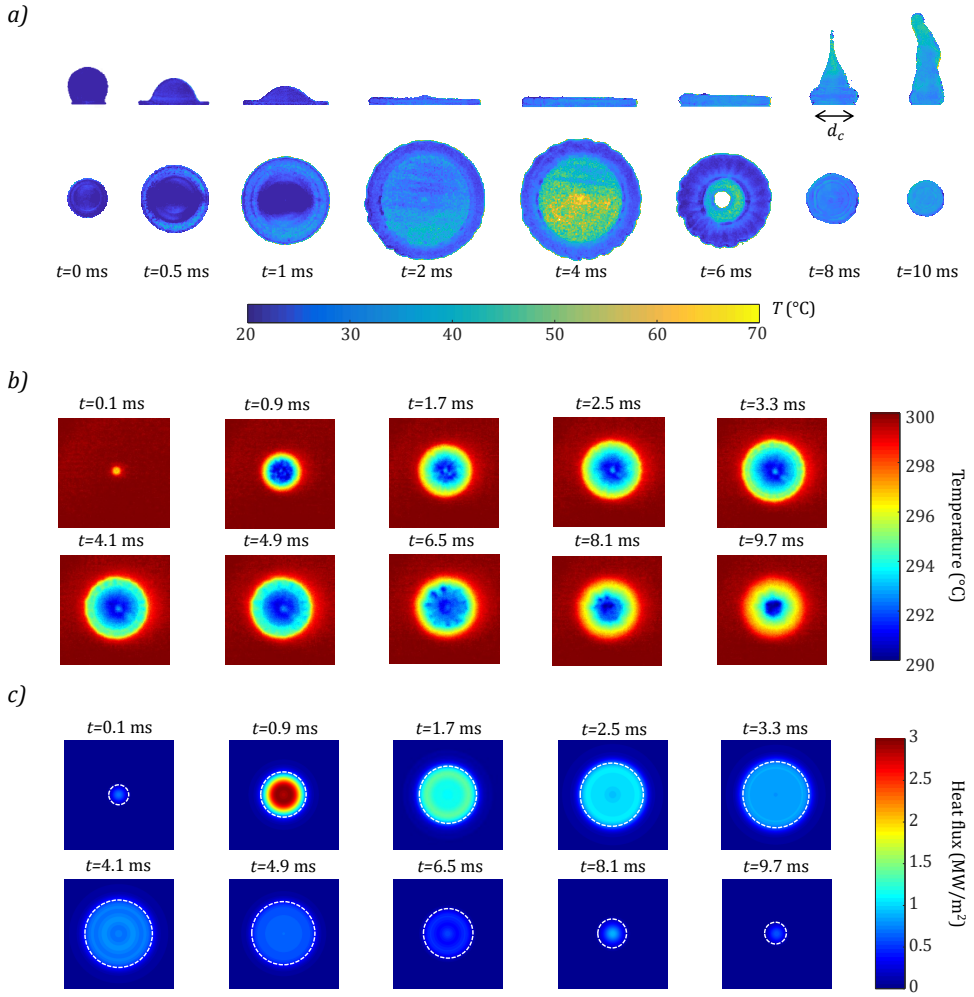


Figure 1. Characterization of heat transfer in the case of an ethanol droplet impinging onto a sapphire window at *We* $= 90$ ($T_{d0} = 20$℃, $T_w = 300$℃, $d_0 = 1.95$ mm). a) Temperature distribution in the liquid drop obtained by 2cLIF imaging. The diameter of the apparent "contact" line d_c can be deduced from the sideview images. b) Temperature distribution at the solid surface measured by infrared thermography. c) Heat flux from the solid surface reconstructed by solving the IHCP. The region of most efficient heat exchange S_e is indicated by the dotted lines.

evaporation, denoted q_v. Breitenbach et al. [8] postulated that the growth rate of the vapor film thickness is directly related to the rate of liquid change into vapor since they considered that $q_v = \rho_l \, Lv \, dh/dt$, where h is the thickness of the vapor film, ρ_l is the liquid density and Lv the latent heat of vaporization. This approximation allows them obtaining an explicit expression for the vapor film thickness without having to involve the momentum balance and the forces acting upon the vapor film. In order to evaluate the theoretical model proposed in the present study, the results from the model are confronted with measurements obtained for ethanol droplets using recently developed optical techniques.

Measurement techniques and experimental observations

A first technique based on two-color laser-induced fluorescence (2cLIF) imaging allows to determine the temperature of the liquid drop during the impact process. Details of the method can be found in Chaze et al. [9]. An example of temperature maps is presented in Fig. 1a. It corresponds to the case of an ethanol drop impinging onto the sapphire window at T_w=300℃ and a value of the Weber number *We* equal to 90. A short time after the beginning of the impact, the droplet takes the shape of a thin lamella of liquid surrounded by an annular rim. In the first times, the heating seems to proceed at a faster rate in the bounding rim, where hot liquid accumulates and mixes with colder liquid already there. As time goes by, the liquid lamella becomes thinner and thinner and the temperature in its inside increases very sharply. The temperature of the lamella gets close to the boiling point of ethanol ($T_{Sat} = 78$℃) at $t = 4$ ms. Nonetheless, the lamella does not account for a significant part of the drop volume at the end of the spreading. The receding of the drop edge accelerates the internal mixing of the liquid. At $t = 10$ ms, the drop leaves the solid surface with a rather uniform temperature, even though the top of the vertically elongated droplet has a slightly higher temperature.

In addition to measuring the droplet temperature , Chaze et al. [10] recently undertook a characterization of the heat flux removed from the hot solid surface. To this end, they used IR thermography. The solid substrate, made of a flat sapphire window, is coated with TiAlN, which is a material very emissive in the IR and resistant to high temperatures.

This work is licensed under a Creative Commons 4.0 International License (CC BY-NC-ND 4.0).

The deposited sub-micron layer of TiAlN is also totally opaque in the IR, and does not modify the thermal impedance of the solid sample. Sapphire being transparent for the wavelengths up to 5 μm-7 μm, the thermal footprint of the droplet on the rear face of the TiAlN deposit can be observed by an IR camera through the opposite face of the sapphire window which is impacted by the droplet. Figure 1b shows a typical set of temperature images recorded with the IR camera. In this example of an impinging ethanol droplet, the cooling of the sapphire surface does not exceed 10℃. An analytical model taking into account the heat conduction in the sapphire substrate was developed to estimate, by an inverse method, the heat flux extracted by the droplet from the solid surface. This model uses the axisymmetry of the polar angle-integrated problem to take advantage of the Hankel transform for a parsimonious parameterization of the variations of temperature and heat flux in the radial direction. This approximation appears to be well justified in Fig. 1b where the temperature distribution on the solid surface seems rather axisymmetric. A maximum of heat flux is reached very rapidly after the beginning of the impact in Fig. 1c, then the heat flux decreases progressively with time. A reliable estimates of the heat flux can be obtained in the film boiling regime, where heat transfer is particularly reduced.

Modeling of the evolution of the vapor film thickness

Given the small thickness of the vapor film, thermal conduction is predominant in the direction perpendicular to the solid surface [8, 11, 6, 7, 12]. As a result, the temperature in the vapor film varies linearly between the liquid surface at the saturation temperature T_{Sat} and the solid surface at $T_{w,s}$. Knowing the value of the heat flux q_w from the resolution of the IHCP, the thickness of the vapor film h can be determined by:

$$h = \lambda_v \cdot \Delta T / q_w, \tag{1}$$

where λ_v is the thermal conductivity of the vapor and $\Delta T = T_{w,s} - T_{Sat}$. Fig. 2 shows profiles of the vapor film at different times corresponding to the same drop impact as in Figs. 1. It can be observed that the vapor film is steadily growing with time until $t \approx 5$ ms, then the thickness increases very rapidly because of the formation of a hole in the middle of the liquid lamella (Fig. 1.a). At t=0.9 ms, the vapor film profile takes a characteristic shape with a bottleneck at the edge. Globally, the difference in thickness between the center and the edge of the film remains very moderate, which justifies the assumption of a uniform thickness of the vapor film made in the following. The

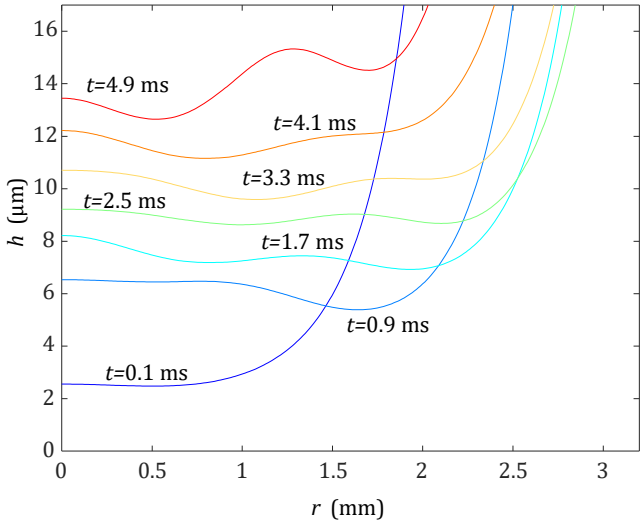


Figure 2. Evolution of the vapor film thickness h for *We* $= 90$ in the case of an ethanol droplet ($T_w = 300$℃, $T_{d0} = 20$℃ and d_0=1.95 mm).

configuration considered for modeling is shown in Fig.3. An axial symmetry is assumed for the problem and the vapor film thickness h is supposed to be uniform but time-dependent. The parameter d_c denotes the diameter of the area of effective interaction between the droplet and the solid surface. It is usually close but not exactly equal to the spreading diameter d_{max}, as the droplet edge is curved.

Flow in the vapor layer- Considering that d_c is, at any time, much larger than h, the problem falls within the scope of the lubrication theory. Taking into account the axisymmetry of the spreading drop, the momentum balance equation in the radial direction r can be expressed as:

$$\frac{\partial v_r}{\partial t} = -\frac{1}{\rho_v}\frac{\partial p}{\partial r} + \nu_v \frac{\partial^2 v_r}{\partial z^2}, \tag{2}$$

where v_r is the radial component of the velocity inside the vapor film and ρ_v and ν_v the density and the kinematic viscosity of the vapor respectively. In this expression, the unsteady term $\partial v_r/\partial t$ is negligible in comparison to the viscous term. A rough estimate for these terms can be made assuming that $\partial v_r/\partial t \sim v_r/t_i$ and $\nu_v \cdot \partial^2 v_r/\partial z^2 \sim \nu_v \cdot$

This work is licensed under a Creative Commons 4.0 International License (CC BY-NC-ND 4.0).

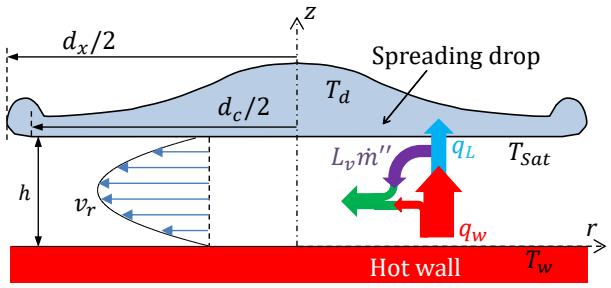


Figure 3. Main features of the model configuration.

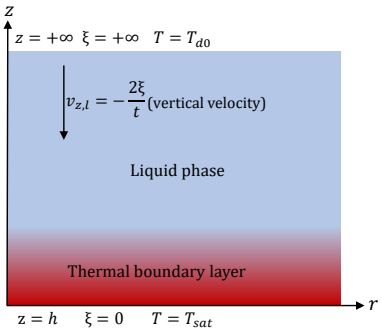


Figure 4. View of the configuration considered for the modeling of the droplet heating.

v_r/h^2, where the characteristic time of an impact t_i is typically a few of ms, $h \sim 1$ μm and $\nu_v \approx 10^{-4}$ m^2/s. Although the thickness of the film h varies with time, the problem can be treated as a quasi-steady one. The mass conservation applied to the vapor film yields:

$$\pi r^2 \dot{m}'' = 2\pi r\, h\, \rho_v\, \bar{v}_r\,(r)\,, \tag{3}$$

where $\bar{v}_r\,(r) = \frac{1}{h}\int_0^h v_r\, dz$ and $\dot{m}''$ is the vapor mass flow rate per unit area. According to Eq.(3), the radial velocity v_r increases linearly with r. This leads to the following velocity field within the vapor layer:

$$v_r = \left(bz + cz^2\right) r \text{ and } v_z = -\int \frac{1}{r}\frac{\partial r v_r}{\partial r} dz = -b\, z^2 - \frac{2}{3} c\, z^3, \tag{4}$$

where b and c are determined in regard to the boundary conditions. When the droplet spreads, a thin liquid lamella bounded by a rim is formed. The flow within this lamella can be approximated by the asymptotic flow solution proposed by Yarin and Weiss.[13]

$$v_{r,l} = \frac{r}{t},\ v_{z,l} = \frac{-2\xi}{t}. \tag{5}$$

where $\xi = z - h$. The subscript l refers to the liquid phase. Eq. (5) corresponds to a non-viscous flow solution. The slip velocity of the liquid/vapor interface is commonly assumed to be not affected by the vapor flow. The liquid drop moves almost freely over the vapor film. Numerous studies have emphasized a significant reduction of friction associated with the presence of a vapor film.[14] In the case of a drop impact, the vapor film is squeezed and the radial velocity v_r of the vapor is usually much larger than the liquid velocity $v_{r,l}$. Therefore, it has been suspected that the liquid can be entrained radially by the vapor flow. In this scenario, according to Castanet et al.[15] the radial velocity at $\xi = 0$ can be determined by:

$$v_{r,l} = \alpha \frac{r}{t} \text{ at } \xi = 0, \tag{6}$$

where α is a parameter that can be slightly larger than 1. The following conditions are considered at the liquid/vapor interface:

$$v_r = v_{r,l} \text{ at } z = h, \tag{7}$$

$$\rho_{v,s} \cdot \left(v_z - \frac{\mathrm{d}h}{\mathrm{d}t}\right) = -\dot{m}'' \text{ at } z = h. \tag{8}$$

In this expression, $\rho_{v,s}$ is the vapor density at the liquid/vapor interface where $T = T_{Sat}$. Using Eqs. (4)-(8), the parameters b and c can be determined by:

$$c = \frac{\alpha}{h^2 t} - \frac{b}{h}, \tag{9}$$

$$b = -\frac{3}{h^2}\left(\frac{\mathrm{d}h}{\mathrm{d}t} - \frac{\dot{m}''}{\rho_{v,s}} + \frac{2}{3}\frac{\alpha\, h}{t}\right). \tag{10}$$

Energy balance- The heat flux taken from the wall q_w is used first to heat up the liquid in the drop, to vaporize the liquid and finally to increase the temperature of the released vapor up to the average temperature in the vapor film which is denoted T_{film}. Hence, the balance of energy flux can be summarized as followed:

$$q_W = q_L + Lv_e \cdot \dot{m}'', \tag{11}$$

where q_L corresponds to the heat flux entering into the liquid drop. This heat flux is responsible for the temperature increase of the droplet during the impact. The parameter Lv_e is introduced with $Lv_e = Lv + (Cp_v \cdot T_{film} - Cp_{v,s} \cdot T_{sat})$ with $Cp_{v,s}$ and Cp_v respectively the heat capacity of the vapor at T_{sat} and T_{film}. Since the variation in temperature in the vapor film is linear along the z-axis, the average temperature of the vapor T_{film} can be well approximated by

This work is licensed under a Creative Commons 4.0 International License (CC BY-NC-ND 4.0).

$T_{film} = (T_{Sat} + T_{w,s})/2$. Using Eqs. (1) and (11), the vapor mass flowrate $\dot{m}''$ can be determined by:

$$Lv_e \cdot \dot{m}'' = \frac{\lambda_v \Delta T}{h} - q_L, \tag{12}$$

Momentum balance- The reaction force F of the vapor film on the impinging droplet is due to pressure inside the vapor film. Using Eq. (4), the integration of Eq.(2) allows obtaining the following expression of the pressure:

$$p\left(r\right) - p\left(r=0\right) = \mu_v \, c \, r^2, \tag{13}$$

On the outer edge of the vapor film at $r = d_c/2$, the pressure returns to the external pressure, meaning that $p = 0$. This yields:

$$p\left(r\right) = \mu_v \, c \cdot \left(r^2 - \frac{d_c^2}{4}\right). \tag{14}$$

The reaction force F can be determined by:

$$F = 2\pi \int_{r=0}^{d_c/2} p\left(r\right) r \, dr = -\frac{\pi}{32} \mu_v \, c \, d_c^4. \tag{15}$$

Using Eqs.(9) and (10), the following expression of the force F can be obtained:

$$F = \frac{3\pi}{32} \mu_v \frac{d_c^4}{h^3} \left(\frac{\dot{m}''}{\rho_{v,s}} - \frac{\alpha \, h}{t} - \frac{\mathrm{d}h}{\mathrm{d}t}\right). \tag{16}$$

This expression of F is equivalent to the Stefan-Reynolds force opposed to the approach of two parallel disks [16] when neglecting the liquid vaporization $\dot{m}''$ and the sliding of the liquid/vapor interface (ie. $\alpha = 0$ and $\dot{m}'' = 0$). Based on Eqs.(12) and (16), the evolution of the vapor film thickness can be determined by solving:

$$\frac{\mathrm{d}h}{\mathrm{d}t} = -\frac{\alpha \, h}{t} + \frac{1}{\rho_{v,s} \, Lv_e} \cdot \left(\frac{\lambda_v \Delta T}{h} - q_L\right) - \frac{32}{3\pi} \frac{h^3 F}{\mu_v d_c^4}. \tag{17}$$

Modeling of the droplet heating

A one-dimensional model for the droplet heating can be associated with the previous description of the vapor film[8]. The droplet is assimilated to a semi-infinite liquid medium (Fig. 3). The thickness of the thermal boundary layer, which develops inside the drop at the interface with the vapor film, is small in comparison to the radial dimension of the spreading drop. Therefore, the thermal gradient in the z direction $\partial T/\partial z$ is dominant relative to that in the radial direction $\partial T/\partial r$. The heat equation can be written:

$$\frac{\partial T}{\partial t} - v_{z,l}\left(\xi\right) \cdot \frac{\partial T}{\partial \xi} = a_l \frac{\partial^2 T}{\partial \xi^2}, \tag{18}$$

where $\xi = z - h$, a_l is the thermal diffusivity of the liquid and $v_{z,l}$ is the z component of the liquid velocity, which can be evalued using Eq.(5). Hence, the convection induced by the liquid flow within the lamella, is taken into account in the equation above. At the liquid/vapor interface, the temperature is imposed by the liquid-vapor saturation:

$$T = T_{Sat}, \text{ at } \xi = 0. \tag{19}$$

Assuming that the thickness of the thermal layer is small compared to the drop thickness, one can expect:

$$T = T_{d0}, \text{ at } \xi \to \infty. \tag{20}$$

where T_{d0} is the drop temperature before impinging onto the hot solid surface. As presented by Breitenbach et al.[8], the above problem can be solved analytically. The temperature field inside the spreading drop is determined by:

$$T\left(\xi, t\right) = T_{Sat} + \left(T_{d0} - T_{Sat}\right) \cdot \mathrm{erf}\left(\frac{\sqrt{5}\,\xi}{2\sqrt{a_l \, t}}\right). \tag{21}$$

The heat flux entering the liquid phase can be calculated from the following expression:

$$q_L = \lambda_l \left.\frac{\mathrm{d}T}{\mathrm{d}\xi}\right|_{\xi=0^+} = C_{q_L} \, t^{-1/2}, \tag{22}$$

$$C_{q_L} = \frac{\sqrt{5} e_l \left(T_{Sat} - T_{d0}\right)}{\sqrt{\pi}}. \tag{23}$$

Here $e_l = \sqrt{\rho_l Cp_l \lambda_l}$ is the thermal effusivity of the liquid. Thus, the increase ΔT_d in the mean temperature of the drop T_m can be evaluated by:

$$\Delta T_d = T_m - T_{d0} = \frac{1}{m \, Cp_l} \int_0^t q_L\left(t\right) \cdot S_e\left(t\right) \mathrm{d}t, \tag{24}$$

This work is licensed under a Creative Commons 4.0 International License (CC BY-NC-ND 4.0).

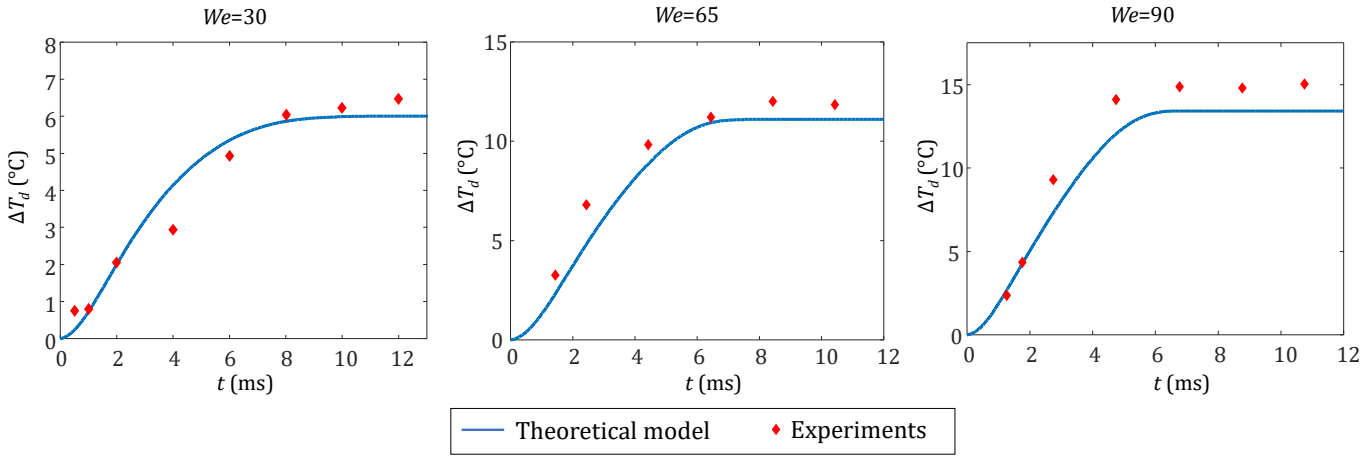


Figure 5. Transient drop heating ΔT_d in the case of ethanol drops impinging onto the sapphire substrate at $T_w = 300$℃ ($T_{d0} = 20$℃, d_0=1.95 mm). Comparison between the model of drop heating and the measurements of the drop temperature by 2cLIF thermometry.

where S_e is the effective surface of heat exchange between the droplet and the solid substrate, i.e. $S_e = \pi d_c^2/4$. The diameter d_c is evaluated from the sideview images taken by laser-induced fluorescence, which allows evaluating the length of the "apparent contact" line between the solid surface and the drop (Fig. 1a). On the hand, it is also possible to estimate the area S_e of most efficient heat transfers directly from the reconstructed distributions of the wall heat flux q_w (Fig. 1c), and then to determine its diameter. These two approaches give roughly equivalent results.
The above-described model of drop heating can be validated against the average temperature in the maps obtained experimentally by laser-induced fluorescence (Fig.1a). The results of this comparison are presented in Fig. 5 in the case of three different values of the Weber number *We*. A good agreement between the experimental data and the results of the theoretical model can be obtained applying Eq. (24). It should be noted that the accuracy of the temperature measurements is of the order of ± 1℃. On the other hand, the temperature calculated from the experimental maps is not rigorously the volume-average temperature (see Ref.[9] for an overview of the measurement biases).

Evolution of the vapor film thickness

To determine the evolution of the vapor film, Eq. (17) has to be solved which implies having a description of the reaction force F and of the "contact" diameter d_c. In the vast majority of applications, the term in F in Eq. (17) can be neglected as it scales in h^3. In addition, F decreases exponentially with time when the drop spreads [17]. Replacing q_L by its expression in Eq. (22) and assuming $F = 0$, the following differential equation can be obtained:

$$\frac{\mathrm{d}h}{\mathrm{d}t} = -\frac{\alpha\, h}{t} + \frac{1}{\rho_{v,s}\, L v_e} \cdot \left(\frac{\lambda_v \Delta T}{h} - \frac{C_{q_L}}{\sqrt{t}} \right). \tag{25}$$

Leaving aside the term $\alpha h/t$, this equation is very similar to that proposed by Breitenbach et al.[8] to describe the evolution of the vapor film thickness. However, an important difference is that the density of the vapor $\rho_{v,s}$ is replaced by the density of the liquid ρ_l (see Eq. 1 p. 37 in Ref.[8]), which introduces an overwhelming influence of the evaporation heat flux q_v in the energy balance. This difference comes from the fact that Breitenbach et al.[8] did not consider exactly the same problem. They assume the situation to be the analog of a vapor/liquid front moving in a semi-infinite liquid medium under the effect of phase change without any regard to pressure forces. An analytical solution of Eq. (25) can be found in the form:

$$h(t) = C\sqrt{t}. \tag{26}$$

Given that $C > 0$, the only possible value of C is determined by:

$$C = \frac{-C_{q_L} + \sqrt{C_{q_L}^2 + (4\alpha + 2)\, \rho_{v,s} L v_e\, \lambda_v \Delta T}}{\rho_{v,s} L v_e \cdot (2\alpha + 1)}. \tag{27}$$

When $C_{q_L}^2 \gg (4\alpha + 2)\, \rho_{v,s} L v_e\, \lambda_v \Delta T$, a Taylor expansion of Eq. (27) to the 1^{st} order with respect to $C_{q_L}^{-1}$ yields:

$$C = \lambda_v\, \Delta T / C_{q_L}\ . \tag{28}$$

This solution implies that the two predominant terms of Eq. (25) are the heat flux taken to the solid surface $q_w = \lambda_v \Delta T/h$ and the heat flux entering the liquid phase $q_L = C_{q_L} \Big/ \sqrt{t}$. Indeed, neglecting the other terms, Eq. (25) is equivalent to:

$$\frac{\lambda_v \Delta T}{h} = \frac{C_{q_L}}{\sqrt{t}}, \tag{29}$$

This work is licensed under a Creative Commons 4.0 International License (CC BY-NC-ND 4.0).

which immediately yields Eq. (28). The above condition $C_{q_L}^2 \gg (4\alpha+2)\,\rho_{v,s} L v_e\,\lambda_v \Delta T$ can be rewritten as:

$$\frac{T_{Sat}-T_{d0}}{T_{w,s}-T_{Sat}} \gg A \cdot \frac{e_v}{e_l}, \tag{30}$$

where $e_v = \sqrt{\rho_v C p_v \lambda_v}$ is the thermal effusivity of vapor and the parameter A is determined by:

$$A = \left[\frac{\pi}{5}(4\alpha+2)\frac{\rho_{v,s}}{\rho_v}\frac{Lv_e}{Cp_v\,\Delta T}\right]^{1/2}. \tag{31}$$

To satisfy the condition in Eq. (30), the initial temperature T_{d0} must be sufficiently low in comparison to T_{Sat}. For example, in the case of an ethanol droplet impinging onto a sapphire substrate at 300℃, parameter A in Eq. (30) is about equal to 3.4, while $e_l \approx 565$ W·K^{-1}· m^{-2}· s$^{1/2}$ and $e_v \approx 9.5$ W·K^{-1}· m^{-2}· s$^{1/2}$ (evaluated at T_{film}). This yields $T_{d0} \ll 64$℃.

Experimental validation of the model in the case of $F = 0$ and a low initial drop temperature T_{d0}

As discussed previously, different cases emerge from the analysis of the evolution of the vapor film thickness. When the liquid drop is sufficiently cold prior to the impact, the condition (30) is satisfied and it is possible to greatly simplify the problem given that $q_L \approx q_w$. In this paper, the focus is on the experimental validation of the model in this limit case. Several experiments were conducted on ethanol droplets injected at the initial temperature of 20℃. The measurements techniques are used to determine both the heat transferred to the droplet Q_L and the heat taken to the solid surface Q_w. The heat energy is evaluated from the measurements of the liquid temperature using the following expression:

$$Q_L = m\,Cp_l\,(T_m - T_{d0})\,, \tag{32}$$

where T_m is the average temperature determined from the measurements by the 2cLIF technique. The heat Q_w is evaluated from the measurements of the solid surface temperature by IR thermography. After determining the heat flux q_w by solving the IHCP, Q_w is evaluated by:

$$Q_w = \int_0^t \int_{S_e(t)} q_w \,\mathrm{d}S\,\mathrm{d}t, \tag{33}$$

where S_e is the cooled surface.

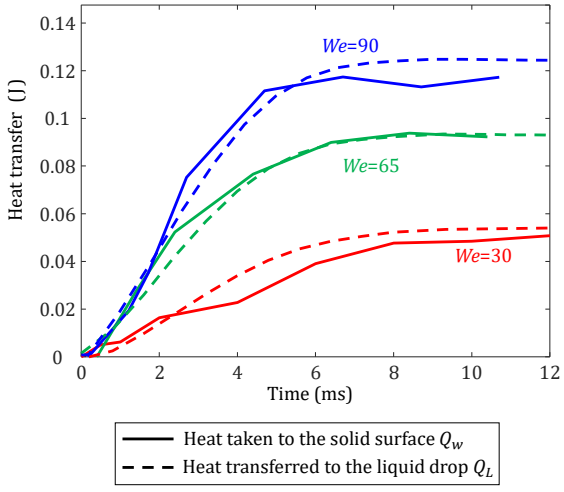


Figure 6. Time evolution of the heat taken to the solid wall Q_W and the heat transferred to the liquid Q_L in the case of an ethanol drop ($T_w = 300$℃ and $T_{d0} = 20$℃).

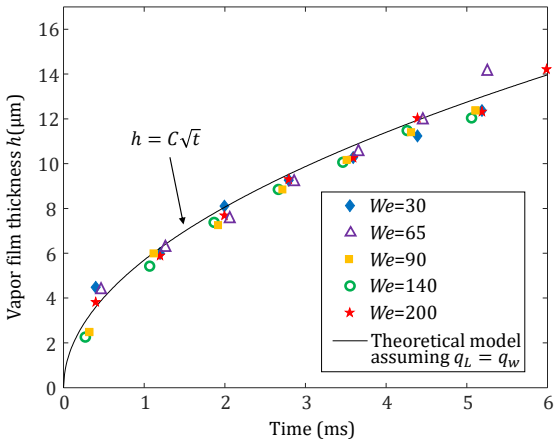


Figure 7. Time evolution of the thickness h of the vapor film for various Weber numbers in the case of an ethanol droplet impinging the sapphire surface ($T_w = 300$℃, $T_{d0} = 20$℃ and d_0=1.95 mm). Comparison to the model based on Eqs.(26) and (28).

Figure 6 displays the time evolution of Q_L and Q_w for different values of the Weber number in the case of an ethanol drop initially at $T_{d0} = 20$℃ and a solid substrate at T_w=300℃. As expected heat transfer increases with *We*, which can be explained by the increase in the spreading surface of the droplet. It is noticeable that Q_w and Q_L are almost equal at any moment of the impact regardless of the Weber number. This confirms that an initial temperature $T_{d0} = 20$℃ is sufficiently low to neglect the contribution of the vaporisation heat flux to the energy balance, as expected from the theory (see the remark after Eq. 31). Of course, measurement errors can affect these experimental data, but it shoud be stressed that they are too weak to change the previous conclusion. Indeed, the drop temperature is determined with an uncertainty of about ± 1℃, which corresponds to an energy of ± 7.2 mJ. The read noise of the infrared camera is about ±0.2℃. Given the axisymmetry assumed for solving the IHCP, pixels at the same distance from the center are averaged altogether to reconstruct the local heat flux, which reduces this error. Furthermore, the measurement noise induced by the parasitic radiations from the sapphire holder is

This work is licensed under a Creative Commons 4.0 International License (CC BY-NC-ND 4.0).

drastically reduced thanks to the deposition of a very emissive coating and the spatial filtering of off-field radiations by the optical system.
Figure 7 shows the time evolution of h for the same impact conditions as in Fig. 6. The thickness of the vapor film seems to be independent on *We*. Estimated values of h are only slightly smaller than the prediction of the theoretical model. For these drops impinging the solid surface at $T_{d0} = 20$℃, the evolution of h is well described by Eqs. (26) and (28), which is consistent with the results presented in Fig. 6 suggesting that $q_w = q_L$.

Conclusions

The evolution of the vapor film thickness has been described in the framework of a quasi-steady approximation, assuming a uniform thickness of the film and one-dimensional heat transfer. A general model for the growth of the vapor film can be obtained from the application of the balance of heat fluxes and the balance of forces applied to the vapor film.
A limit case of the model is obtained when the temperature of the drop before impact is low compared to the saturation temperature of the liquid. In the case of this "cold" drop, heating of the drop outweighs the heat used for the evaporation of the liquid. The growth of the film is governed solely by the rate at which the drop heats up. The impact velocity has no effect on the vapor film. Very simple expressions can be obtained for the evolution of the vapor film thickness and the decrease in temperature of the solid surface. They are validated by experiments conducted on ethanol drops at several Weber numbers.

Acknowledgements

The authors gratefully acknowledge the financial support of the ENERBATIN CPER program and the European FEDER program.

References

[1] Y. Ji, N. Nagai, K. Takano, Effect of inclination angle onto heat transport characteristics of bubble-actuated circulating heat pipe covering high-temperature region, in: 15^{th} International Heat Transfer Conference, 2015, p. 119334.
[2] B. J. Kim, K. D. Kim, Effect of initial temperature of a cylindrical steel block on heat transfer characteristics of staggered array jets during water jet quenching, Heat Transfer Engineering 36 (12) (2015) 1037–1045.
[3] J. Kim, Spray cooling heat transfer: The state of the art, International Journal of Heat and Fluid Flow 28 (4) (2007) 753–767.
[4] R. Rioboo, C. Tropea, M. Marengo, Outcomes from a drop impact on solid surfaces, Atomization and Sprays 11 (2).
[5] I. V. Roisman, E. Berberović, C. Tropea, Inertia dominated drop collisions. i. on the universal flow in the lamella, Physics of Fluids 21 (5) (2009) 052103.
[6] A.-L. Biance, C. Clanet, D. Quéré, Leidenfrost drops, Physics of Fluids 15 (6) (2003) 1632–1637.
[7] B. Sobac, A. Rednikov, S. Dorbolo, P. Colinet, Leidenfrost effect: Accurate drop shape modeling and refined scaling laws, Phys. Rev. E 90 (2014) 053011.
[8] J. Breitenbach, I. V. Roisman, C. Tropea, Heat transfer in the film boiling regime: Single drop impact and spray cooling, International Journal of Heat and Mass Transfer 110 (2017) 34 – 42.
[9] W. Chaze, O. Caballina, G. Castanet, F. Lemoine, Spatially and temporally resolved measurements of the temperature inside droplets impinging on a hot solid surface, Experiments in Fluids 58 (8) (2017) 96.
[10] W. Chaze, O. Caballina, G. Castanet, J.-F. Pierson, F. Lemoine, D. Maillet, Heat flux reconstruction by inversion of experimental infrared temperature measurements - Application to the impact of a droplet in the film boiling regime, International Journal of Heat and Mass Transfer 128 (2019) 469–478.
[11] Y. Guo, K. Mishima, A non-equilibrium mechanistic heat transfer model for post-dryout dispersed flow regime, Experimental Thermal and Fluid Science 26 (6) (2002) 861 – 869.
[12] B. Sobac, A. Rednikov, S. Dorbolo, P. Colinet, Self-propelled leidenfrost drops on a thermal gradient: A theoretical study, Physics of Fluids 29 (8) (2017) 082101.
[13] A. L. Yarin, D. A. Weiss, Impact of drops on solid surfaces: self-similar capillary waves, and splashing as a new type of kinematic discontinuity, Journal of Fluid Mechanics 283 (1995) 141–173.
[14] J. D. Berry, I. U. Vakarelski, D. Y. C. Chan, S. T. Thoroddsen, Navier slip model of drag reduction by leidenfrost vapor layers, Physics of Fluids 29 (10) (2017) 107104.
[15] G. Castanet, O. Caballina, F. Lemoine, Drop spreading at the impact in the leidenfrost boiling, Physics of Fluids 27 (6) (2015) 063302.
[16] J. Stefan, Versuch über die scheinbere adhäsion, Sitzungsberichte der Mathematisch-naturwissenschaften Klasse der Kaiserlichen Akademie der Wissenschaften, II. Abteilung (1874) 713–735.
[17] I. V. Roisman, E. Berberović, C. Tropea, Inertia dominated drop collisions. i. on the universal flow in the lamella, Physics of Fluids 21 (5) (2009) 052103.

This work is licensed under a Creative Commons 4.0 International License (CC BY-NC-ND 4.0).